

MACHINE LEARNING PREDICTION MODEL FOR SMALL DATA SETS INSTEAD OF DESTRUCTIVE TESTS FOR A CASE OF RESISTANCE BRAZING PROCESS VERIFICATION

Nemanja Pajić¹, Marko Djapan¹, Eva Buluschek², Waldemar Fahrenbruch³, Aleksandar Đorđević^{1,*},
and Miladin Stefanović¹

¹Faculty of Engineering
University of Kragujevac
Kragujevac, Serbia

*Corresponding author's e-mail: adjordjevic@kg.ac.rs

²Faculty of Information Systems and Applied Computer Sciences
Otto-Friedrich-Universität
Bamberg, Germany

³Faculty of Automotive Technology
Hochschule Coburg
Coburg, Germany

This paper presents a case study of Machine Learning (ML) prediction model for small data sets instead of destructive testing of brazed contacts. The main problems noted in the study were data availability, data quality, an extremely low number of NOK destructive test results and overall small data set. Recent researches are not very often focused on small data set ML prediction models and even less often on its application in resistance brazing. This paper tends to bridge this gap. The case study methodology consists of data collection, data preparation, correlation analysis, feature selection, model training, hyperparameter optimization, and model evaluation. It is proven possible to train ML prediction model with small datasets to predict numerical test outcomes if dataset quality is adequate. The practical use of this approach is reflected in the reduction of test costs since destructive tests can be quite expensive, and ML prediction model is one time, relatively low investment.

Keywords: Non-Destructive Testing, ML, Hard Soldering, Small Data Sets, Quality Prediction.

(Received on November 2, 2022; Accepted on March 30, 2023)

1. INTRODUCTION

When it comes to quality, product safety, and dependability, the automotive sector is among the most demanding of all industries (Misokefalou *et al.*, 2022). In unreliable or high-risk manufacturing processes, it is necessary to test each and every component. If the production process is stable, repeatable and reproducible but it is linked to some special characteristic of the product, statistical process control (SPC) might be applied (Kumpati *et al.*, 2021). All the tests are non-value-adding; hence they increase the production cost of the product. If tests are destructive, this means that a product is lost for this test, thus increasing the costs even more. Some destructive tests are requested by a customer, some are necessary in order to have a better insight in the process quality and/or adjust production parameters, and some destructive tests are linked to special characteristics with a high potential risk (Siwiec and Pacana, 2021). Destructive testing requires trained staff, expensive equipment, time and supplies, and of course, a product to be destroyed (Maev *et al.*, 2021).

This study is focused on a real-life project of destructive test substitution with a ML prediction model, for brazing process verification, in the plant of one of Tier 1 automotive suppliers. In this study, SPC is represented by destructive testing of electric drive stators to verify the brazed contact quality between the copper coil and the phase ring. The analyzed product is a three-phase electric drive stator, with copper coils resistance brazed on the phase rings (Figure 1). The specified test utilizes a randomly selected stator from the manufacturing process to assess the parameters of the brazed contact and the needed pull force to separate the contact. The stator is cut, and brazed contacts are separated. Some brazed contacts are used to test the pull force, and some are grinded, polished and observed under the microscope (Figure 2). Under the microscope, cross-section width and height are measured, and cracks and voids are looked for. These tests are utilized as a way of statistical

process control and a method of production release. The market share of electric and hybrid cars is growing. Therefore, the manufacturing of electric drives is becoming increasingly important (Husain *et al.*, 2021). Electric drives may be rather expensive. Therefore, destructive testing can incur a great deal of unnecessary expenses. Replacing destructive testing with non-destructive alternatives might result in considerable cost savings. If the manufacturing process is stable, fewer components should be examined. In the project implementation phase, the testing frequency needs to be high until there is sufficient data to decide whether the process is reliable or not. In addition, an SPC destructive test cannot ensure that 100% of the manufactured components meet the specifications. Also, in the test described in this study, a cross-section cut is performed on the contact and observed under the microscope, which may easily be done in a defect-free region of a defective contact, hence incorrectly classifying the defective product as a part with no defects. Having all these limitations of destructive SPC testing in mind, a better solution is required.

1.1 Brazing process and destructive testing process verification description

Figure 1 depicts a three-phase electric drive stator with 24 copper coils that have been firmly soldered (resistance brazed) to three-phase copper rings. Brazing is a category of hard soldering joining procedures in which filler material (solder) is heated over 450°C (above the filler's melting point) (Sevryukov *et al.*, 2015). There are four primary heating techniques for brazing: torch or manual brazing, induction brazing, resistance brazing, and vacuum brazing (Weis *et al.*, 2017). Resistance brazing is seldom mentioned in contemporary scientific literature. Most of the research papers in the past few years have been focused on advancements of brazing filler materials, brazing of dissimilar materials, and novel methods for utilization of existing brazing technology (Ahn, 2021; Sevryukov *et al.*, 2015; Weis *et al.*, 2017). This paper focuses on Cu-Cu resistance brazing with basic filler materials (Figure 1).

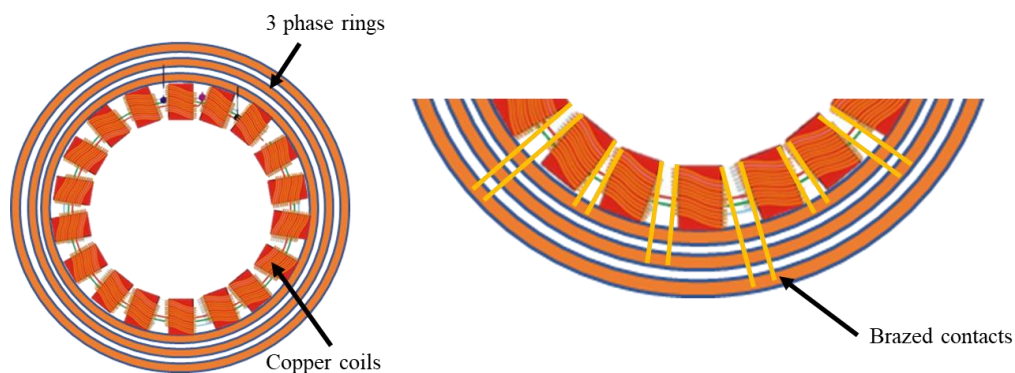


Figure 1. Graphic presentation of the stator in question and brazed contacts on 3 phase rings (adapted from Chen *et al.*, (2009))

The brazing head consists of 2 brazing probes, which can separately move along the Z axis. Copper wires are laid on a phase ring that already contains brazing added material, and the current is passed through the probes. Due to resistance heating and pressure, the added material melts, the wire flattens, and a secure connection is made between the wires and a phase ring, as shown in Figure 2.

If the process parameters are not set up correctly, there is a risk of gas bubbles forming, which may lead to voids in the brazed region; fractures may also arise; wire may be crushed or not squeezed sufficiently; and a great number of other flaws may also occur. Problems of a similar kind may manifest themselves if the brazing region contains any contaminants. These kinds of flaws have the potential to have a major impact on the brazed contact's thermal and electrical conductivity, as well as on its lifetime and dependability (Wankerl *et al.*, 2020).

Presently, destructive testing entails slicing off individual brazed contacts to examine them closely using a microscope (Figure 3). The height and length of a wire's cross section are measured, and any flaws, such as pores or fractures, are examined. In the last 3 years, in quality reports of the production plant in which the project was done, cracks and voids were only detected in fewer than 1% of SPC test samples and in less than 0.000003% of all manufactured parts; hence this study focuses on predicting wire width and height. Since the analyzed sample data showed that the process was extremely stable, this choice was made since there was not enough data to educate the algorithm with.

An additional test is being performed on the same tested unit to save the cost of the destroyed part, a pull-off test. Different contact is rigged in a pull-off tester to determine the tearing force. Test results are documented manually in an Excel sheet and stored as a PDF on SharePoint.

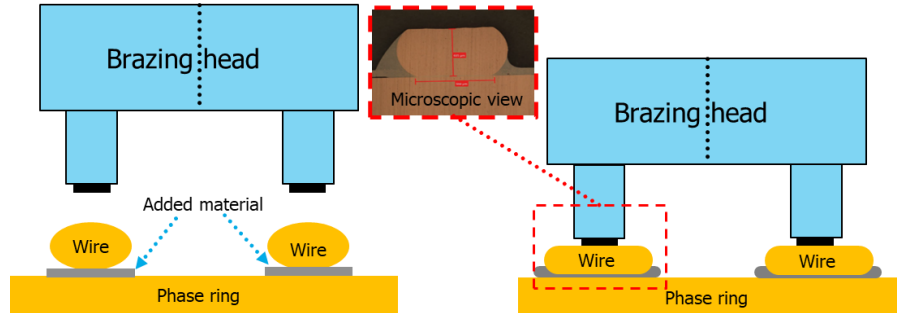


Figure 2. Schematic representation of the brazing process with a microscopic view of a brazed area cross-section (adapted from Mookam (2019))

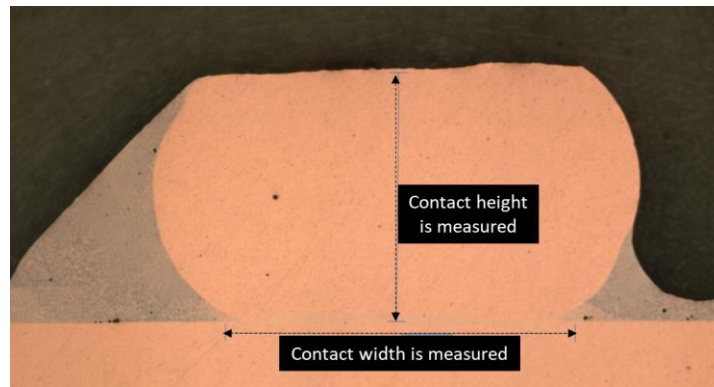


Figure 3. Microscopic view of a brazed area cross-section (created by authors)

1.2 Modern Non-Destructive Testing

In the recent past, there was a technological barrier limiting the use of some Non-Destructive Testing (NDT) solutions. In some cases, NDT methods took a lot of time, which was not suitable for in-line testing (Machado *et al.*, 2022). Some NDTs require a high testing equipment investment, thus, are limited for the top-level suppliers. In the past, the automotive industry did not prioritize the development of NDT solutions since they may hinder production (Nöthen, 2021). In today's unpredictable economic situation, numerous modern NDT procedures are applicable in the automotive sector, establishing new directions and trends with great reliability and efficiency (Ding *et al.*, 2022; Machado *et al.*, 2022, 2021). To avoid unnecessary losses and testing costs (testing time, materials, equipment, manpower, etc.), various modern non-destructive testing (NDT) methods have been studied. The most common non-destructive methods are (Madupu *et al.*, 2017; Nöthen, 2021): ultrasonic testing, magnetic particle testing, penetrant testing, thermography, eddy current testing, X-Ray/Computed Tomography (CT), and Artificial intelligence (AI) – ML. Some of these methods are more suitable for the required application than the others. Each of these methods has its advantages and disadvantages.

As a very effective and versatile technique, ultrasonic testing can pinpoint the precise position of defects and even reveal slight differences in the material's structure, even on the smallest of components, though it might not be reliable for objects smaller than 1.2mm and probe and the tested component must be separated by a coupling fluid or gel (Ding *et al.*, 2022). Ultrasonic transducers can withstand 150°C for a couple of seconds, and the brazing process usually occurs in an environment above 500°C. Thus, some researchers (Vasilev *et al.*, 2021) presented a novel contactless ultrasonic approach for working with 3 mm steel sheets utilizing air as the coupling medium, while others (Lalithakumari and Pandian, 2020) utilized an AI approach (such as Deep learning) to improve interpretation of the ultrasonic test results and increase test reliability. Ultrasonic testing might not be the best approach because of the small size of brazed contacts and potential defects and a short time for testing in line (2 seconds per joint).

Another non-destructive method that is frequently used is magnetic particle testing (MPT). However, MPT proved unsuitable for in-line testing of such tiny copper components with stringent cleaning requirements. MPT is a technique for detecting fractures or flaws in ferromagnetic materials by adding the ferromagnetic powder to an item and generating a magnetic field around it. Copper is diamagnetic (and in certain circumstances paramagnetic), and a stator is full of crevices where the powder might dwell, hence preparation and cleaning would be required for the test to maintain a high degree of cleanliness; therefore, this approach is not appropriate to the given study (Singh, 2020).

In penetrant non-destructive testing, the part must be cleaned and dried. It is necessary to apply the penetrant, remove any surplus penetrant, and wait for the reaction to take place after some time has passed (Guirong *et al.*, 2015). After this process, the part should be visually inspected. The examination might also be done using a camera, but this method is time-consuming, has the potential to contaminate the item, and, consequently, unable to identify cavities inside the brazed contact. (Guirong *et al.*, 2015). With this in mind, penetrant testing is not suitable for this application for mostly the same reasons as MPT.

Thermography involves the use of a flash lamp for the purpose of stimulating the material being examined and an infrared (IR) camera for the purpose of inspecting the materials for flaws (Kumar and Reddy, 2018). During the joining process (soldering, welding, brazing, etc.), heat may be created using passive thermography, and a thermal camera is used to identify any faults. It is a fast and reliable testing method, suitable for high temperature environments and large components. Since the equipment for fast in-line testing can be relatively expensive, a brazing station could not fit thermography equipment without significant modification and scanning on a different location requires line modification and customer approval, hence this option wasn't chosen (Kumar and Reddy, 2018; Siegel *et al.*, 2020).

With the development of technology, eddy current non-destructive testing has emerged. It has been shown that eddy current testing may efficiently find faults as minor as a few microns (cracks, voids, delamination, etc.) in a very prompt manner (a couple of milliseconds test interval). Eddy current testing uses an excitation coil that induces a magnetic field and receiver coils that pick up the signal of induced eddy current in the tested part (Machado *et al.*, 2021). This testing technique was considered a leading contender; nevertheless, for most of the same reasons that were given for thermography, it was not selected as the final approach.

X-Ray and Computed Tomography (CT) can provide significant insight into the brazed area, detect defects of a couple of microns in size, measure the size of the part or the defect, and also CT can provide a 3D measurement of the part and much more (Galos *et al.*, 2021; Hamade and Baydoun, 2019). CT and X-Ray scanners can produce high-quality test results, but this method requires trained staff, expensive equipment, dedicated testing space, and a dedicated, specific computer, and it usually takes a lot of time to analyze the results (Wankerl *et al.*, 2020; Xiao *et al.*, 2021). Equipment is very expensive, even for laboratory use, but for in-line testing with space limitations, a fast-paced process, short testing time and high scanning resolution requirements, the equipment price goes even higher. Due to the high material mix of the product and high material density, this approach proved to be very challenging in real-life applications, as it was tested by researchers.

ML prediction models can be applied to predict the outcome of certain production processes. If the ML prediction model is "fed" with the data from the production process (process parameters, i.e., pressure, temperature, voltage...) and destructive test results (wire cross-section dimension, defect presence, pull force, etc.), various algorithms can be applied to form a prediction for future production (Badora *et al.*, 2021). Once an ML model is optimized for a certain process and model training is completed with historical data (process data and destructive test result data), it can be successfully applied to monitor the production process of the new parts and predict a hypothetical destructive test result (Kumar *et al.*, 2022). ML model, if well trained, could predict not only a class (OK or Not OK) but a specific value of the test result, such as wire width, height, defect presence, etc. (Buongiorno *et al.*, 2022). This approach can be used to minimize or, if possible, completely substitute destructive testing. If destructive testing is by any means required, the ML prediction model could help choose the parts which are most likely to be NOK ones (Not OK – nonconform part). The advantages of this method compared to destructive testing are numerous. The ML prediction model can control 100% of produced parts. It is a one-time investment, faster, reduces health and safety hazards, and a solution is transferable to different production plants with low to no additional costs... Substitution of destructive testing of brazed contacts with ML leads to savings in terms of time and money, improves product and process insight, reduces potential health and safety hazards, can be applied to test 100% of the parts, and a solution is transferable to different production plants with low to none additional costs and much more.

1.3 Content of the study and Literature gaps

This study is focused on the development of a ML prediction model which is supposed to predict an outcome of a destructive test using solely brazing process parameters without destruction of the part. The paper provides an explanation of quality processes, focusing on SPC in a form of destructive and Non-Destructive test methods. An overview of modern NDT methods has been given. A short explanation of the brazing process and destructive test in question is also provided. The main part of

this case study consists of data collection, data preparation, ML method shortlisting, correlation analysis, feature selection, model training, hyperparameter optimization, and model evaluation.

The limited amount of literature sources on topics such as Non-Destructive Testing of brazed contacts, ML prediction of the result of the brazing process, and ML prediction model for small data sets served as the motivation for this research. Available research is mostly focused on laser welding and big data ML prediction models with a considerable amount of NOK test results (Breitenbach *et al.*, 2021; Faragó *et al.*, 2022; Hong *et al.*, 2022; Rong *et al.*, 2016; Shevchik *et al.*, 2020; Zhou *et al.*, 2020). Laser welding is most often analyzed through optical backlash imaging, which is a completely different approach of ML, based on visual input and image recognition (Shevchik *et al.*, 2019). This study focuses on the small data set of process parameters (voltage, resistance, temperature, etc.) with extremely low number of failed test results. Big data and small data sets require completely different ML algorithms, and low amount of NOK test results makes model training much more difficult (Badora *et al.*, 2021; Ji *et al.*, 2022; Zhang and Ling, 2018). This can also be considered as a gap in literature since most of the research papers are focused on ML applications on Big Data sources where data sets can have a 50-50% ratio of OK and failed test results. (Kokol *et al.*, 2022). When using small datasets in ML prediction models, it is usually much more difficult to train the model and reach a satisfactory effectiveness level of the model compared to Big Data analytics (Kokol *et al.*, 2022). Overall, small datasets with a low number of NOK values are more challenging compared to Big data analytics and require a different approach, different algorithms and a model training process (Kokol *et al.*, 2022; Sendek *et al.*, 2022).

2. MATERIALS AND METHODS

This chapter, as shown in Figure 4, will present the following: the process of data collection and description, data restrictions, data preparation and hyperparameter optimization, and feature selection. First, the collection of data (process parameters and test results) was done. In the data preparation step, data was converted, filtered, translated, and formatted using the Knime analytics platform. Once data was set, certain data restrictions and limitations were identified. Having data prepared and its limitations known led to the step of finding proper ML methods (4 methods were shortlisted). Once the ML methods were shortlisted, feature selection, model training and hyperparameter optimization were done for all 4 methods. Finally, the results were analyzed, and models evaluated.

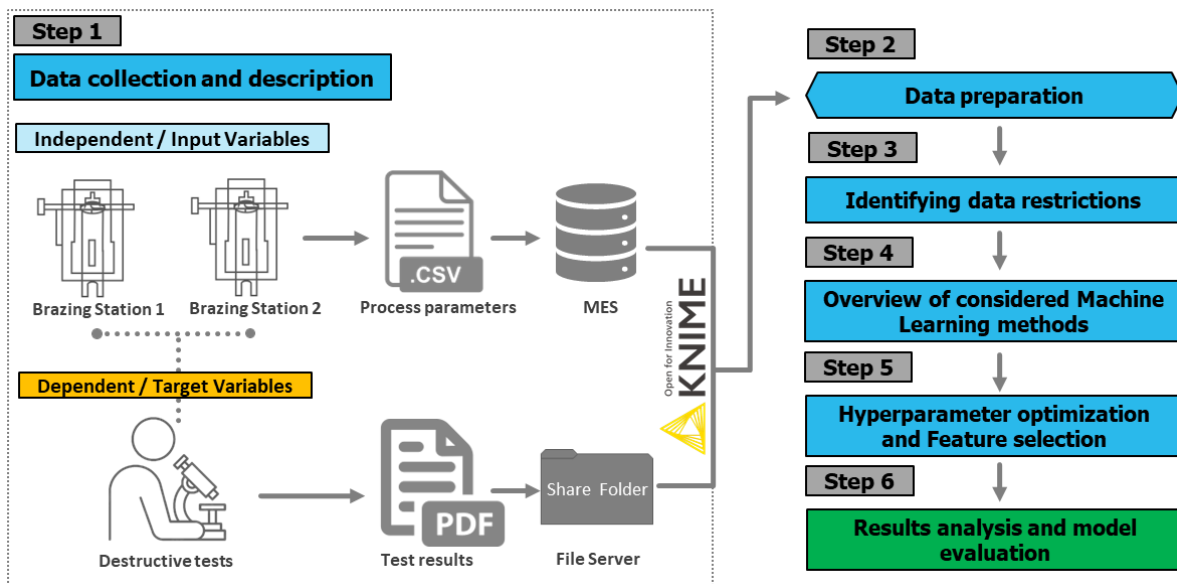


Figure 4. Graphical representation of process of data collection and description; data restrictions; data preparation; and hyperparameter optimization and feature selection (created by authors)

2.1 Data collection and description

The data considered as input in this study originate from the manufacturing process of e-drive stators. Two identical automated brazing stations linked to a manufacturing execution system (MES) database give the input data. Measurements such as the yield path of the left and right probe, average voltage, average current, brazing duration, the temperature of the

left and right probe, and brazing status are recorded for each of the 24 coils that make up the stator. The pressing force of the probe is not a real-time measurable value but rather a value that is predetermined. If this information was available, the outcomes of predictions could be much more accurate. If any of the measurements lie beyond the lower or upper specification limits, the produced part is of status “fail” and is not considered for further destructive testing during regular serial production. In summary, the input dataset consists of measurement data of 134,535 unique serial numbers with status “pass” and 2,765 serial numbers with status “fail”.

The target data is obtained from test methods that record destructive macro analysis and pull test readings. Each protocol contains the following test results:

- Soldering height in micrometers at 12 locations on the stator (two coils per long, medium, and short distance from interconnector) for two sides each (left and right)
- Soldering width in micrometers at 12 locations on the stator (two coils per long, medium, and short distance from interconnector) for two sides each (left and right)
- Pull test results in Newton on 6 locations
- Existence of cracks in the wires that are not filled with solder on 6 locations
- Wire indentation (only measured if present) at 6 locations

In total, the target dataset consists of 688 protocols with status “pass” and 10 protocols with status “fail” within a time frame of 32 months. Data collection corresponds to step 1, shown in Figure 4.

2.2 Data preparation

Data preparation, model training and evaluation are performed in the KNIME Analytics Platform (Berthold *et al.*, 2008, 2020). The destructive testing protocols had to be converted from PDF to Excel format using batch conversion in a PDF editing program to make them machine-readable before loading them into KNIME, whereas the input data was directly accessed from KNIME via a database connection. This also corresponds to step 2, shown in Figure 4.

Data cleaning steps included removing input and target columns with more than 10% missing data as well as columns with low variance. After joining on the unique part identifier (the serial number), the resulting dataset consisted of 585 rows, 168 numerical input features (brazing parameters), and 30 numerical and 15 categorical target features (test results). Since 15 categorical features can be categorized only with OK and NOK status, and in more than 99% of the tests, all tested features were OK, they were excluded from the prediction model.

From this combined dataset, a 70:30 train-test split was performed using stratified sampling based on the input brazing station number.

2.3 Data restrictions

Since macro analysis and pull tests are destructive testing methods, the target dataset is small in comparison to the input dataset and thus limits the range of possible ML algorithms to choose from without leading to overfitting. The target dataset is also highly imbalanced, with only 1.4% of the parts failing the test. Therefore, the decision was made to formulate the ML task not as a classification to predict the overall outcome of the destructive test but as a regression targeting the individual measurements, which can then be interpreted in conjunction with the existing specification limits. For pull-off test results, it was documented only if the part was OK (conform part) or NOK (Not OK- nonconform part). Test results do not contain information about the force the part withstood, nor which force was sufficient to tear it. The information available teaches the algorithm only if certain process parameters lead to an OK or NOK part on the pull-off test.

In addition, the manual nature of the test protocols complicated the ingestion process: The PDF file format required additional transformation steps to make the protocols machine-readable; the non-standardized format meant that sometimes fields were not consistently filled the same way, and lastly, the differing languages (input data: German, target data: Serbian) and the alphabet made additional translation steps necessary. PDF conversion corresponds to step 3, shown in Figure 4.

The data-entering process also led to some considerable data quality challenges: The content of two columns was switched for some test protocols, some entries had missing digits (e.g., “163” instead of “1163”), and errors in the primary key entry “serial number” led to records which could not be matched to the input data. This led to some additional manual data-cleaning efforts.

2.4 Overview of considered ML methods

There are very few research articles that concentrate on the application of ML to brazing processes in general, and there are even fewer or none that specifically focus on resistance brazing. Having in mind that ML models applied to similar processes

(i.e., laser welding) have proven to be an effective and efficient method of process verification, a review of different ML methods was conducted in order to find suitable ones (Faragó *et al.*, 2022; Rong *et al.*, 2016; Shevchik *et al.*, 2020)

Because both the input data (process parameters) and the output data (the results of the destructive test) were accessible in the scenario that was presented, supervised learning algorithms were selected as the method of choice for further study. The overview of ML methods corresponds to step 4, shown in Figure 4. Supervised learning involves data that has been assessed and then modified with additional information to monitor the ML algorithm. It is just a matter of providing data in sufficient quantities, which are already stored with the correct function value. In such a case, one speaks of "labeled (marked) data sets" (Frochte, 2021). Furthermore, supervised learning is divided into two sections – classification and regression. In classification, predefined categories or classes are assigned to each item (Jo, 2021). That means that in classification problems, the output value of the target class is discrete. Regression estimates an output value based on multiple input factors (Jo, 2021). In regression problems, the output is continuous. As the available labeled data set is small, the choice of the best ML method for small data sets is considered as a further selection criterion. At the same time, one must consider various pitfalls in the data sets. Essentially, training data is a composite of two components: signal + noise.

Considering the signal component as the main information in data and simultaneously the noise component as undefined, highly volatile data, the overfitting and underfitting concepts can be easily understood (Jiang, 2021). In the case where a model is too simple to catch all conditions of the signal, the trained model will give poor results. This case is called underfitting (Jiang, 2021). On the other hand, a complex model will try to catch all of the noise in the given data and will abstract the model from fitting all regularities from the signal. By using a complex model, the noise component can highly influence and deflect the training outcome (Jiang, 2021). According to the project criteria and data availability, various methods were analyzed and chosen.

Linear regression is a simple and effective machine-learning method. Furthermore, it can be well applied to small data sets, and its results may be intuitively interpreted (Jiang, 2021). Generally, if at least approximately a correlation between two characteristics in a population is suspected, linear regression calculation can be used to investigate and specify the correlation. For this purpose, two characteristics of interest, X and Y, are tested on objects from the population (Hartung *et al.*, 2005). The $2n$ realizations x_1, \dots, x_n and y_1, \dots, y_n will be used to investigate the linear connection as presented in Equation 1:

$$y = \alpha + \beta x_i + e_i \text{ for } i = 1, \dots, n, \quad (1)$$

where α is the absolute term, and β is the slope parameter of the linear relationship. As mentioned above, there are often failures or misleading information in the data, described as noise. The parameter e_1, \dots, e_n represents the noise in this equation (Hartung *et al.*, 2005). To determine the point estimates a and b for the parameters of α and β of a linear regression problem, in such a way that by regression line shown in Equation 2:

$$\hat{y} = a + bx. \quad (2)$$

The best possible estimate \hat{y} for the expression of y of the characteristic Y, which has the expression x of the characteristic X, is determined (Hartung *et al.*, 2005). As criterion for the quality of the estimation, the sum of the deviation squares is used as a measure, as shown in Equation 3:

$$R^2 = \sum_{i=1}^n (y_i - a - bx_i)^2 \quad (3)$$

The estimators a and b for α and β must be determined in such a way that the sum of R^2 of the vertical squared deviations of the measured values y from the provided values for x in the regression line $y_i - a - bx_i$ becomes minimal. This method is called method of least squares (Galos *et al.*, 2021). Pseudocode for Linear Regression is shown in algorithm 1 as an example.

Algorithm 1 Linear Regression pseudocode (Strehl and Littman, n.d.)

0: **Inputs:** a, β

1: Initialize $x = [x_1, \dots, x_n]$ and $y = [y_1, \dots, y_n]$ and number of observations n.

2: Compute $S_x = \sum_{i=1}^n x_i$ and $S_y = \sum_{i=1}^n y_i$

3: Initialize sum of product of x and y S_{x*y}

4: Initialize sum of square of x S_{x*x}

5: **for** $i = 1, 2, 3, \dots : n$ **do**

6: Compute S_{x*y} as $S_{x*y} = \sum_{i=1}^n x_i * y_i$

- 7: Compute S_{x*x} as $S_{x*y} = \sum_{i=1}^n x_i * x_i$
- 8: Compute β as $\beta = \frac{(n*S_{x*y} - S_x*S_y)}{(n*S_{x*x} - S_x*S_x)}$
- 9: Determine mean values $meanX$ and $meanY$
- 10: Compute α as $\alpha = meanX - \beta * meanY$

In algorithm 1 $x = [x_1, \dots, x_n]$ represent independent variable values, $y = [y_1, \dots, y_n]$ represent dependent variable values; S_x sum of all values for the observed independent variable x ; S_y sum of all values for the observed dependent variable y at the level of each observation i ; S_{x*x} sum of all squared values for the observed independent variable x at the level of each observation i ; S_{x*y} sum of all product values for the observed independent variable x and dependent variable y at the level of each observation i , α estimated intercept and β estimated slope.

Random Forest and Gradient Boosted Trees both belong to the tree-based models. Both methods combine the outputs from individual decision trees. Based on the evaluation of neural networks, random forest, regression trees and support vector machines, decision-tree-based algorithms show easier application in the training (Rodriguez-Galiano *et al.*, 2015). The main advantage of Gradient boosted trees is the method of boosting, which sequentially combines weak decision trees, the so called weak learners, so that in the new decision tree, the errors of the previous ones are corrected. Avoiding the overfitting by learning from simple data sets, as the weak learners are not capturing all complex dynamics in the data, is a further advantage. Considering tabular data, in some cases, supervised learning methods, like Gradient Boosted Tree Regression, even outperform the nowadays popular Deep Learning methods (Shwartz-Ziv and Armon, 2021). Algorithm 2 shows pseudocode for Gradient boosted tree as an example.

Algorithm 2 Gradient boosted tree pseudocode (Qi et al., 2018)

- 1: **Inputs:** $D = \{(x_1, y_1), \dots, (x_N, y_N)\}$, θ , γ
- 2: **Output:** $F(x) = \sum_{i=0}^M F_i(x)$
- 3: Initialize $F_0(x) = \arg \min_{\beta} \sum_{i=0}^N L(y_i, \beta)$
- 4: **While** ($m < M$)
- 5: $d_i = -[\partial L(y_i, F(x_i)) / \partial F(x_i)]$ $F(x_i) = F_{m-1}(x_i)$
- 6: $\vartheta = \{(x_i, d_i)\}, i = 1, N$
- 7: $g(x) = \text{FITREGRETREE}(\vartheta, \theta)$
- 8: $\rho_m = \arg \min_{\rho} \sum_{i=1}^N L(y_i, F_{m-1}(x) + \rho g(x))$
- 9: $F_m(x) = F_{m-1}(x) + \gamma \rho_m g(x)$
- 13: **End while**

In the Random Forest method, different decision trees are built and parallelly combined. In comparison to other ML techniques, for the Random Forest, only two parameters are required to generate a model: the amount of regression trees and the amount of evidential features (Jiang, 2021). Reducing the number of evidential features brings, as a result, a reduction in the correlation among trees, which increases the model's accuracy (Rodriguez-Galiano *et al.*, 2015). The pseudocode for the Random Forest method is shown as an example in Algorithm 3.

Algorithm 3 Random Forest pseudocode (Guo et al., 2021)

- 1: To generate c classifiers:
- 2: **For** $i = 1$ to c **do**
- 3: Randomly sample the training data D with replacement to produce D_i
- 4: Create a root node, N_i containing D_i
- 5: Call Build Tree (N_i)
- 6: **End for**
- 7: **Build Tree (N):**
- 8: **If** N contains instances of only one class **then**
- 9: **Return**
- 11: **Else**
- 12: Randomly select $x\%$ of the possible splitting features in N
- 13: Select the feature F with the highest information gain to split on
- 14: Create f child nodes of N , N_i, N_f , where F has f possible values (F_1, \dots, F_f)
- 15: **For** $i = 1$ to f **do**
- 16: Set the contents of N_i to D_i , where D_i is all instances in N that match F_i


```

17:     Call Build Tree ( $N_i$ )
18: End for
19: End If

```

Kernel Ridge Regression, also called Kernel Ridge Squares, was taken into consideration as a further ML model, as only a small number of the destructive test results were available (Stulp and Sigaud, 2015) (Zhang and Ling, 2018). This method uses the advantage of the kernel function, which projects the data set in a higher dimensional space by transforming the features of a data set. The basic idea behind bringing the data set into a higher dimensional space by transforming the original features is to reorganize the geometry of the original features to have more trivial geometry of the feature of the data set (Jung, 2022). The two kernels considered are a linear kernel and a radial basis function kernel. Furthermore, Kernel Ridge Regression is a non-linear regression form with an overfitting prevention regularization (Vu *et al.*, 2015). In algorithm 4 pseudocode of Kernel Ridge Regression is shown.

*Algorithm 4 Kernel Ridge Regression pseudocode (Liu *et al.*, 2022)*

```

0: Input: stored populations of the preceding time steps  $\{P^1, P^2, \dots, P^t\}$ ,  $P_k = \{v_{ij}^k \mid$ 
0:  $i=1, 2, \dots, N; j=1, 2, \dots, d; k=1, 2, \dots, t\}$ ;
0: Output: initial population of the new time step  $P^{t+1} = (v_1^{t+1}, \dots, v_N^{t+1})$ ;
1: for  $i=1, \dots, N$  do;
2:   for  $j=1, 2, \dots, d$  do
3:     generate a time series  $s = (v_{ij}^1, v_{ij}^2, \dots, v_{ij}^t)$  from the stored populations;
4:     obtain training samples from  $s$  by using sliding window technique;
5:     use training samples to train a KRR model;
6:     set test instance  $x^{t+1} = (v_{ij}^{t-q+1}, \dots, v_{ij}^t)$ ;
7:     predict the label value ( $v_{ij}^{t+1}$ ) of the test instance; according to  $y^T (K + \alpha I_q)^{-1} \kappa$  derived from (Liu et al., 2022)
8:     repair  $v_{ij}^{t+1}$  if it is out of the boundary value according to [4];
9:   end for
10: end for

```

2.5 Hyperparameter optimization and Feature selection

With a training set size of only 409 rows and 168 input features, there is an increased risk that a ML algorithm will find patterns that are not valid for the general population (Jensen and Shen, 2008). Therefore, a Forward Feature Selection loop was implemented to pre-select a set of input features for the training of the Linear Regression model; this corresponds to step 5, shown in Figure 4. For each target variable, the number of features was optimized by maximizing the evaluation metric “Adjusted R-squared”, which penalizes the addition of irrelevant input variables to the model; this corresponds to step 5, shown in Figure 4 (Devore, 2012).

Table 1. Overview of Hyperparameter Optimization Settings

Model	Optimization Method	Model Parameter	Optimization parameters
Random Forest Regression	Grid Search	nr_models	Start: 50 Stop: 200 Step size: 10
Random Forest Regression	Grid Search	max_depth	Start: 1 Stop: 31 Step size: 2
Gradient Boosted Tree Regression	Grid Search	max_depth	Start: 2 Stop: 10 Step size: 2
Gradient Boosted Tree Regression	Grid Search	learning_rate	Start: 0.1 Stop: 1.0 Step size: 0.1
Kernel Ridge Regression (Linear Kernel)	Grid Search	alpha	Start: 0.1 Stop: 1.0 Step size: 0.1

Model	Optimization Method	Model Parameter	Optimization parameters
Kernel Ridge Regression (RBF Kernel)	Bayesian Optimization (TPE)	alpha	Start: 0.1 Stop: 1.0 Max_iterations: 100 Warm up: 40 Gamma: 0.25 No_candidates: 25
Kernel Ridge Regression (RBF Kernel)	Bayesian Optimization (TPE)	gamma	Start: 0.00005 Stop: 0.1 Max_iterations: 100 Warm up: 40 Gamma: 0.25 No_candidates: 25

Table 1 shows an overview of which hyperparameter optimization techniques have been applied for each ML algorithm. These methods were implemented using the KNIME Parameter Optimization Loop in connection with 2-fold cross-validation.

For model hyperparameter optimization and overall model evaluation, the coefficient of determination R^2 (“R-squared”) was used. This coefficient expresses the proportion of the variance in the target variable, which is predictable from the input variables and has been implemented in the form of the KNIME (Berthold *et al.*, 2008) Numeric Scorer node.

3. RESULTS AND DISCUSSION

In this section, correlation analysis will be shown along with regression model results. Also, the general benefits of this approach will be discussed.

3.1 Correlation Analysis

Correlation analysis was performed to measure the strength of the linear relationship between process parameters and destructive test measurements. This corresponds to step 3, shown in Figure 4. It yielded some strong correlations between the brazing parameters “yield path” and the macro analysis measurements of “height after soldering” and “solder width” for identical coils on the stator. These findings confirm the production logic outlined in Section 1.

It was identified that, in general, macroanalysis failures are not visible outliers when considering macroanalysis measurements but could be found in the center of the distribution, as Figure 5 shows. Additionally, in Figure 5 can be seen that when the yield path increases, solder width also increases. Figure 6 shows the same behavior for pull test failures. Additionally, in Figure 6, we can see that when the yield path increases, solder height decreases. Figure 7 differentiates between the two twin brazing stations. The difference in distribution was present for almost all measurements and led to the decision to use stratified sampling in the train-test split for model training. In Figure 7, it is possible to see that there are no significant differences between the two stations, thus no additional steps are required.

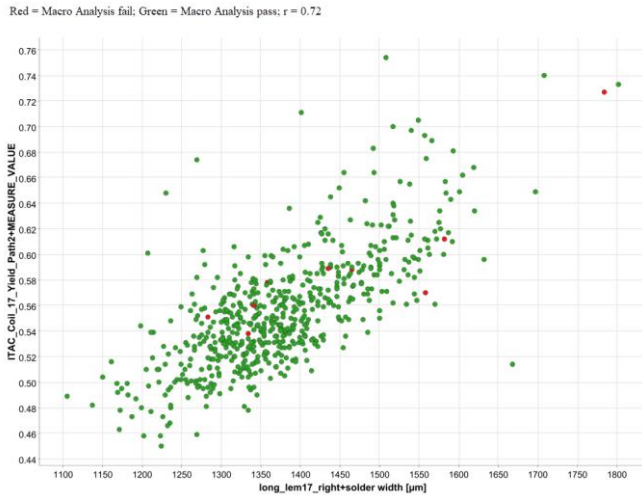


Figure 5. Scatterplot of correlation between brazing parameters and macroanalysis measurement. Red = Analysis failed, green = analysis pass. $r = 0.72$

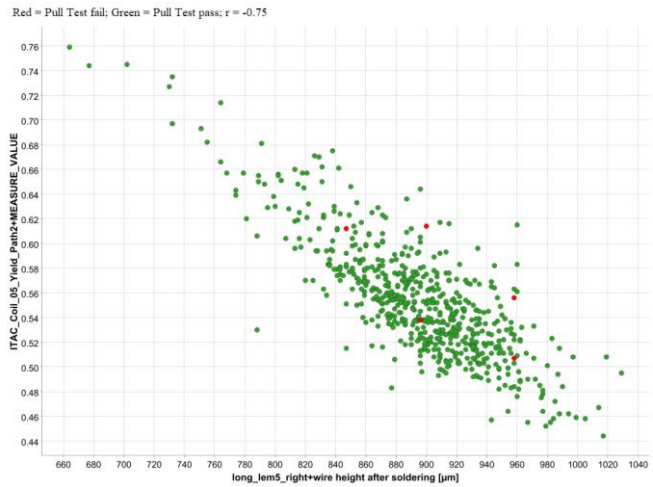


Figure 6. Scatterplot of correlation between brazing parameters and macroanalysis measurement. Red = Pull test failed, green = Pull test pass. $r = -0.75$

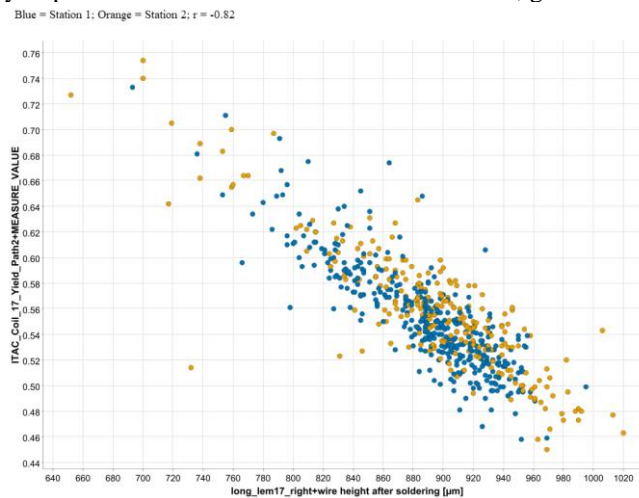


Figure 7. Scatterplot of correlation between brazing parameters and macroanalysis measurement. Blue = Brazing station 1, orange = Brazing station 2. $r = -0.82$

3.2 Regression Model results

In total, for 19 out of 30 numeric target variables, a model performance with an R^2 value of 0.5 or higher was achieved. Out of those 19, Linear Regression performed the best for 11, Linear Kernel Ridge Regression for 4, Gradient Boosted Tree Regression for 3, and Random Forest Regression for 1. A comparison of all model results per target can be seen in Table 2.

It can be seen from Table 2 that there is a significant difference between the prediction performance of the macroanalysis measurements and the pull test results. None of the models were able to reliably predict the force under which the wire will break when being pulled. It is also noteworthy that Kernel Ridge Regression was never the top-performing model in any of the cases with an R^2 value above 0.5. This subsection corresponds to step 6, shown in Figure 4, model evaluation.

Table 2. Model evaluation results: Gradient Boosted Regression (GB), Kernel Ridge Regression (KRR) Linear Regression (LR), Random Forest Regression (RF), KRR with Radial Basis Function Kernel (KRR_RBF)

Target	GB R2	KRR R2	LR R2	RF R2	KRR RBF R2	Max R2	Max model
<i>medium_lem1 9_left+wire height after soldering [μm]</i>	0.723	0.692	0.815	0.703	0.078	0.815	LR
<i>long_lem1 7_right+wire height after soldering [μm]</i>	0.789	0.722	0.792	0.652	0.401	0.792	LR
<i>long_lem5_right+wire height after soldering [μm]</i>	0.747	0.696	0.761	0.604	0.075	0.761	LR
<i>long_lem1 7_left+wire height after soldering [μm]</i>	0.675	0.669	0.698	0.732	0.379	0.732	RF
<i>short_lem1 8_left+wire height after soldering [μm]</i>	0.571	0.605	0.713	0.665	0.055	0.713	LR
<i>short_lem1 8_right+wire height after soldering [μm]</i>	0.519	0.327	0.668	0.242	0.317	0.668	LR
<i>long_lem5_left+wire height after soldering [μm]</i>	0.618	0.524	0.668	0.575	0.085	0.668	LR
<i>long_lem1 7_right+solder width [μm]</i>	0.664	0.575	0.594	0.526	0.174	0.664	GB
<i>medium_lem1 9_left+solder width [μm]</i>	0.639	0.644	0.659	0.328	0.574	0.659	LR
<i>long_lem5_right+ solder width [μm]</i>	0.629	0.605	0.655	0.585	0.513	0.655	LR
<i>long_lem1 7_left+solder width [μm]</i>	0.626	0.645	0.506	0.322	0.459	0.645	KRR
<i>medium_lem1 7_right+wire height after soldering [μm]</i>	0.635	0.645	0.637	0.639	0.131	0.645	KRR
<i>medium_lem1 9_right+wire height after soldering [μm]</i>	0.615	0.591	0.641	0.616	0.243	0.641	LR
<i>long_lem5_left+solder width [μm]</i>	0.622	0.567	0.542	0.538	0.315	0.622	GB
<i>short_lem6_left+wire height after soldering [μm]</i>	0.569	0.416	0.611	0.600	-0.002	0.611	LR
<i>short_lem1 8_left+solder width [μm]</i>	0.330	0.609	0.604	0.572	0.442	0.609	KRR
<i>medium_lem1 7_left+wire height after soldering [μm]</i>	0.574	0.489	0.607	0.568	0.261	0.607	LR
<i>short_lem6_left+solder width [μm]</i>	0.568	0.500	0.434	0.237	0.026	0.568	GB
<i>medium_lem1 7_left+solder width [μm]</i>	0.532	0.559	0.469	0.303	0.472	0.559	KRR
<i>short_lem6_right+wire height after soldering [μm]</i>	0.439	0.454	0.486	0.431	0.138	0.486	LR
<i>medium_lem1 7_right+solder width [μm]</i>	0.455	0.446	0.423	0.481	0.371	0.481	RF

Figure 8 shows predicted vs. actual value line plots of wire height for the target with the highest R² (0.815), in this case, predicted by the Linear regression method. Even though the small data set was analyzed, and process parameter data was limited and lacked some crucial information (such as the pressure of the probe on contact), it was sufficient to reliably predict the dimensions of the contact cross-section. Since the cutting room technician always cuts the same contacts for the standard destructive test (contacts: 9, 10, 11, 21, 22 and 23) and the other contacts only on a specific demand. This means that there was much more data for some contacts than others. This fact didn't have a great influence on the prediction results.

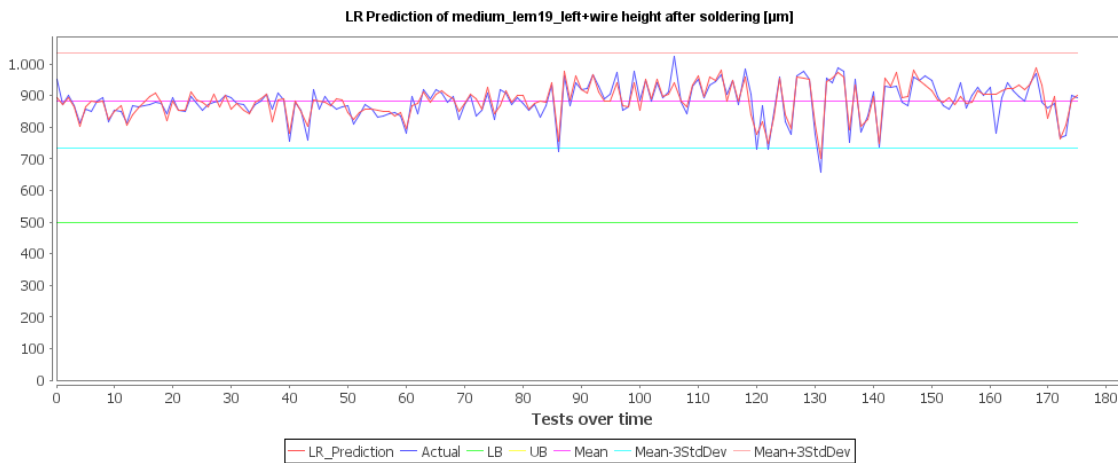


Figure 8. Predicted vs. Actual value line plots of wire height for the target with the highest R² (0.815)

Figure 9 shows that even for the worst-performing macroanalysis target model, the predicted values are not significantly close to the specification limit. In Figure 10, it can be seen that the process is stable and well above the lower specification limit of 700μm (green line). From the practical point of view, even if the prediction results were not so precise, it would be safe for this specific process to use the ML prediction model as a process monitoring method.

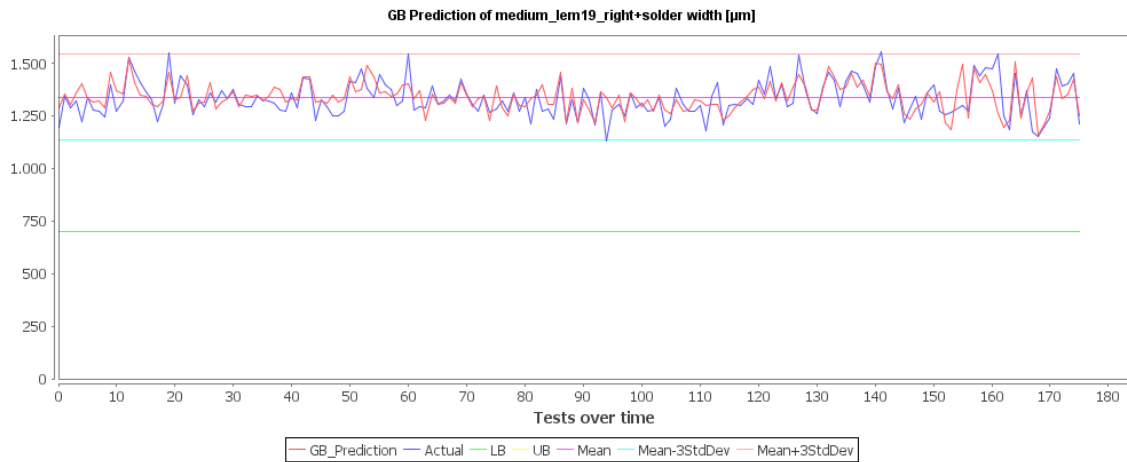


Figure 9. Predicted vs. Actual value line plots of the worst macroanalysis wire width target (R^2 0.426)

Figure 10 shows predicted vs. actual value line plots of the highest pull test result (R^2 0.296). Pull test result data was very limited. The test shows the force on which the wire broke or which force it withstood. Nevertheless, it was not documented in the test results. The only information available in the test result about the pull test is if the part is OK or NOK.

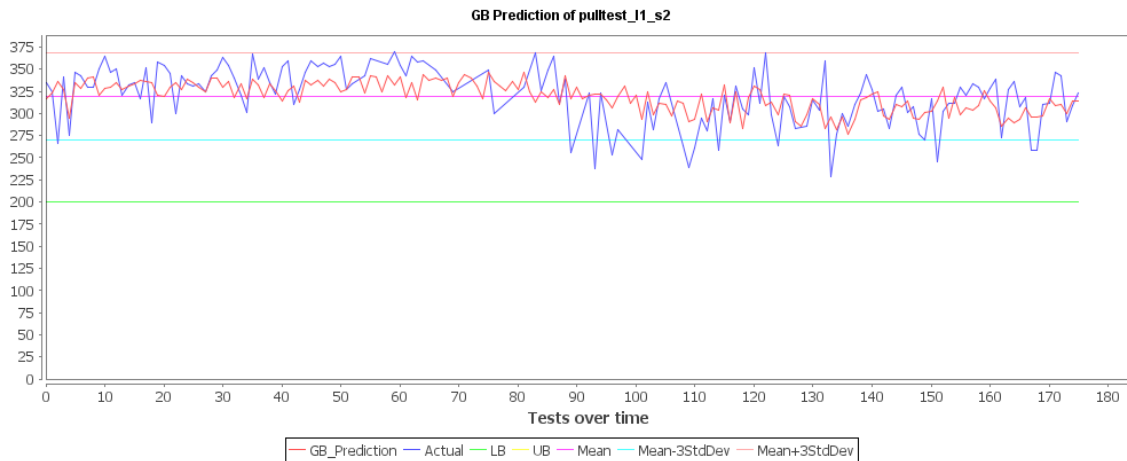


Figure 10. Predicted vs. Actual value line plots of the highest pull test result (R^2 0.296)

Lacking this numerical value, it was very hard to predict the pull test result in a numerical term. Since the process is stable, there were not that many variations and all predicted results were in the correct zone (zone of OK parts). It can therefore be concluded that while pull test predictions are not reliable, and macroanalysis results can be predicted by the ML model.

3.3 Benefits of the ML prediction approach

The general idea was to train the model to predict wire width and height, the presence of cracks and voids, and the pull force required to tear a contact. If all these ML predictions were possible, destructive tests could be aborted or minimized. This would lead to significant savings in time, test cost, and reduction of health and safety risks; it would enable 100% testing inline, and the tested part would be saved. In the current scenario of destructive tests, the stator needs to be produced, brought to the laboratory, documented, then cut, ground, polished, and observed under the microscope; a report must be created, and the sample part needs to be scrapped. On the other hand, the ML prediction model would be integrated into the production line with no nonvalue-adding activity required to test the part. All results would be almost instantly stored in the plant’s software system.

Due to specified project and data limitations, the ML prediction model was not fully capable of substituting destructive tests. Pull test results could not be predicted in a precise manner since data contained only information if the sample passed the destructive test or not, but not the actual pull force value. The goal was to predict a numerical value, not a class (OK or NOK). Cracks and voids could not be predicted since an extremely low number of these defects was represented in the dataset. Wire width and height of the brazed contact cross-section were predicted in a satisfactory way.

With the results obtained during an experiment, some improvements could be done. Since statistical testing controls only a fraction of the entire production, it is better to test the worst possible part than any random part. With limited prediction capabilities, the ML algorithm could be used to separate/suggest critical parts which are to be submitted to destructive testing. This is beneficial in two ways. Firstly, if ML predicts suspicious parts, it is much cheaper and more time efficient to test them in the plant than to send them to the customer and receive a claim. Claim management might include sorting activities abroad, recall of the parts, penalties for stopping the production line of the customer, decreased supplier rating, and for sure, a lot of time of the local engineering team which is handling the claim. Secondly, if the worst part is submitted to the destructive test, we could learn if the production process parameters need to be optimized. Additionally, when a complete electric motor is assembled and tested on the EOL (end of line), defects of the brazing process on the stator might be uncovered. This means that there is a possibility of destroying a good part for testing in the laboratory and then scraping another one on EOL.

Even with the limited capabilities, this prediction model could be something to benefit from in the production. As more data is collected with time, the algorithm will be retrained, and it will increase in effectiveness. The solution is easily transferable to multiple locations in the world with similar production processes with virtually no investment except data mining and data wrangling on each specific site. Other destructive and NDT methods would require a relatively high investment in testing equipment. With time, better ML methods may appear, providing better results than those obtained in this experiment. It is highly important to set the course for future development. Having in mind that AI and ML can be very beneficial if correct data of proper quality is provided, it is necessary to plan for the future. Production processes and test results must be designed in such a way that will provide the right kind of data to AI in the near future.

4. CONCLUSIONS

In production of a relatively expensive product, destructive tests may incur high financial losses. Non-destructive testing (NDT) methods offer a solution to this issue by reducing testing costs significantly. While state-of-the-art NDT technologies can provide excellent testing results, not all methods are applicable to every use case. For this particular use case, the goal was to develop a non-destructive testing solution with a 100% testing frequency in-line solution, a short ROI period, and high transferability to other projects and locations. Some testing methods require a significant financial investment, such as CT scanners, while others are not suitable for in-line testing due to fast-paced production, such as ultrasonic testing. Additionally, some methods carry a risk of product contamination, such as magnetic particle or penetrant testing, while others require a long implementation time and production station reconstruction, such as eddy current testing. Finally, some methods cannot provide the measurement resolution necessary for the given application. In this use case, a ML prediction model was determined to be the best fit for the project requirements.

It is proven possible to predict brazed contact width and height, which are typically correlated to the input features. Macroanalysis tests could probably be replaced by ML prediction, given the distance from the specification limits. Pull force could not be precisely predicted due to missing information about the process and destructive test results. Brazing probe pressing force is critical information for this process, and it is a set value, not real-time measured. Destructive test results do not contain information about the pull force value but only information if the test was OK or NOK.

Four different ML prediction models were used on a small dataset to predict the brazing process outcome and test results. ML methods were shortlisted based on the given application, having in mind that the data set is very small and the failed test reports are extremely rare. Methods applied in this case study were Linear Regression, Linear Kernel Ridge Regression, Gradient Boosted Tree Regression, and Random Forest Regression. Out of 30 numerical values tested, 19 had an R^2 value of 0.5 or higher. Out of those 19, Linear Regression performed the best for 11, Linear Kernel Ridge Regression for 4, Gradient Boosted Tree Regression for 3, and Random Forest Regression for 1. Based on the results, Linear Regression performed best with the given dataset.

To achieve satisfactory results, the input data must be sufficient (meaning it must include process-defining parameters and contain enough values) of high quality and well formatted. The given data set contained 98% of OK test results and less than 2% of failed test results. This ratio is very limiting and challenging. A better data ratio could probably lead to higher prediction accuracy, leaving this as a topic for future research. If some of the process-defining value measurements are lacking (such as probe pressing force), that is also reducing the success rate of the prediction model. The same limitations apply to the missing values from the test reports (such as the pull force value). Small datasets are limiting but can lead to a successful prediction model, but lack of process or test defining data/values renders success rate significantly.

The limited literature available on topics such as Non-Destructive Testing of brazed contacts, ML prediction of brazing process outcomes, and ML prediction models for small data sets served as the impetus for this research. However, most of the available research is focused on laser welding and big data ML prediction models, with a considerable amount of NOK (not-okay) test results. While laser welding is often analyzed through optical backlash imaging, which relies on visual input and image recognition, ML algorithms for big data and small data sets require different approaches. Moreover, the low amount of NOK test results in small datasets makes model training much more challenging. This gap in the literature highlights the need for more research on ML applications for small datasets with low NOK values, which require different algorithms and model training processes compared to big data analytics. Overall, such datasets are more challenging to work with and require a different approach.

Future research can be developed in multiple directions. Primarily AI and ML prediction models for small datasets should be researched. Various industrial processes could benefit from AI prediction models but are limited with small datasets. Developing new algorithms or improving existing ones could be beneficial. Various NDT techniques for the outcome prediction of resistance brazing processes (or welding in general) could be enhanced with AI, i.e., in terms of test result interpretation for better test effectiveness and efficiency. One of the strategic points for future research would be product, process, and test design for easy integration of AI prediction models. It is important to have in mind which data will be necessary from newly designed products/processes/tests in a year or two when there is enough data to train ML prediction models.

REFERENCES

- Ahn, B. (2021). Recent Advances in Brazing Fillers for Joining of Dissimilar Materials. *Metals*, 11: 1037. DOI: <https://doi.org/10.3390/met11071037>
- Badora, M., Sepe, M., Bielecki, M., Graziano, A., and Szolc, T. (2021). Predicting Length of Fatigue Cracks by Means of ML Algorithms in The Small-Data Regime. *Eksploatacja I Niezawodność*, 23(3): 575-585. DOI: <https://doi.org/10.17531/ein.2021.3.19>.
- Berthold, M., Borgelt, C., Höppner, F., Klawonn, F., and Silipo, R. (2020). *Guide to Intelligent Data Science: How to Intelligently Make Use of Real Data (Second Edition)*. Texts in Computer Science. Springer. DOI: <https://doi.org/10.1007/978-3-030-45574-3>.
- Berthold, M. R., Cebron, N., Dill, F., Gabriel, T. R., Kötter, T., Meinl, T., Ohl, P., Sieb, C., Thiel, K., and Wiswedel, B. (2008). KNIME: The Konstanz Information Miner. in C. Preisach, H. Burkhardt, L. Schmidt-Thieme, & R. Decker (Eds.), *Data Analysis, ML and Applications, Studies in Classification, Data Analysis, and Knowledge Organization* (Pp. 319-326). Springer Berlin Heidelberg. DOI: https://doi.org/10.1007/978-3-540-78246-9_38.
- Breitenbach, J., Dauser, T., Illenberger, H., Traub, M., and Buettner, R. (2021). A Systematic Literature Review on ML Approaches for Quality Monitoring and Control Systems for Welding Processes. in *2021 IEEE International Conference on Big Data (Big Data)* (Pp. 2019-2025). IEEE. DOI: <https://doi.org/10.1109/bigdata52589.2021.9671887>.
- Buongiorno, D., Prunella, M., Grossi, S., Hussain, S. M., Rennola, A., Longo, N., Di Stefano, G., Bevilacqua, V., and Brunetti, A. (2022). Inline Defective Laser Weld Identification by Processing Thermal Image Sequences with Machine and Deep Learning Techniques. *Applied Science*, 12: 6455. DOI: <https://doi.org/10.3390/app12136455>.
- Chen, A., Rotevatn, N., Nilssen, R., and Nysveen, A. (2009). Characteristic Investigations of A New Three-Phase Flux-Switching Permanent Magnet Machine by FEM Simulations and Experimental Verification. in *2009 International Conference on Electrical Machines and Systems* (Pp. 1-6). IEEE. DOI: <https://doi.org/10.1109/icems.2009.5382791>.
- Deepak, J. R., Bupesh Raja, V. K., Srikanth, D., Surendran, H., and Nickolas, M. M. (2021). Non-Destructive Testing (NDT) Techniques for Low Carbon Steel Welded Joints: A Review and Experimental Study. *Materials Today Proceedings*, 44: 3732-3737. DOI: <https://doi.org/10.1016/j.matpr.2020.11.578>.
- Deng, H., Cheng, Y., Feng, Y., and Xiang, J. (2021). Industrial Laser Welding Defect Detection and Image Defect Recognition Based on Deep Learning Model Developed. *Symmetry*, 13: 1731. DOI: <https://doi.org/10.3390/sym13091731>.
- Devore, J. L. (2012). *Probability and Statistics for Engineering and The Sciences* (8th Ed.). Brooks/Cole, Cengage Learning.

- Ding, L., Lu, Q., Liu, S., Xu, R., Yan, X., Xu, X., Lu, M., and Chen, Y. (2022). Quality Inspection of Micro Solder Joints in Laser Spot Welding by Laser Ultrasonic Method. *Ultrasonics*, 118: 106567. DOI: <https://doi.org/10.1016/j.ultras.2021.106567>.
- Faragó, K. B., Skaf, J., Forgács, S., Hevesi, B., and Lőrincz, A. (2022). Soldering Data Classification with A Deep Clustering Approach: Case Study of An Academic-Industrial Cooperation. *Applied Sciences*, 12: 6927. DOI: <https://doi.org/10.3390/app12146927>.
- Frochte, J. (2021). *Maschinelles Lernen: Grundlagen Und Algorithmen in Python* (3rd Ed.). Hanser, München.
- Galos, J., Ghaffari, B., Hetrick, E. T., Jones, M. H., Benoit, M. J., Wood, T., Sanders, P. G., Easton, M. A., and Mouritz, A. P. (2021). Novel Non-Destructive Technique for Detecting The Weld Fusion Zone Using A Filler Wire of High X-Ray Contrast. *NDT & E International*, 124: 102537. DOI: <https://doi.org/10.1016/j.ndteint.2021.102537>.
- Guirong, X., Xuesong, G., Yuliang, Q., and Yan, G. (2015). Analysis and Innovation for Penetrant Testing for Airplane Parts. *Procedia Engineering*, 99: 1438-1442. DOI: <https://doi.org/10.1016/j.proeng.2014.12.681>.
- Guo, H., Nguyen, H., Vu, D.-A., and Bui, X.-N. (2021). Forecasting Mining Capital Cost for Open-Pit Mining Projects Based on Artificial Neural Network Approach. *Resources Policy*, 74: 101474. DOI: <https://doi.org/10.1016/j.resourpol.2019.101474>.
- Hamade, R. F., and Baydoun, A. M. R. (2019). Nondestructive Detection of Defects in Friction Stir Welded Lap Joints Using Computed Tomography. *Materials & Design*, 162: 10–23. DOI: <https://doi.org/10.1016/j.matdes.2018.11.034>.
- Hartung, J., Elpelt, B., and Klösener, K.-H. (2005). *Statistik: Lehr- Und Handbuch Der Angewandten Statistik; Mit Zahlreichen, Vollständig Durchgerechneten Beispielen* (14., Unwesentlich Veränd. Aufl. Ed.). Oldenbourg.
- Hong, Y., Yang, M., Jiang, Y., Du, D., and Chang, B. (2022). Real-Time Quality Monitoring of Ultra-Thin Sheets Edge Welding Based on Micro-Vision Sensing and SOCIFS-SVM. *IEEE Transactions on Industrial Informatics*, 1–11. DOI: <https://doi.org/10.1109/tii.2022.3199258>.
- Husain, I., Ozpineci, B., Islam, M. S., Gurpinar, E., Su, G.-J., Yu, W., Chowdhury, S., Xue, L., Rahman, D., and Sahu, R. (2021). Electric Drive Technology Trends, Challenges, and Opportunities for Future Electric Vehicles. *Proceedings of The IEEE*, 109: 1039–1059. DOI: <https://doi.org/10.1109/jproc.2020.3046112>.
- Jensen, R., and Shen, Q. (2008). *Computational Intelligence and Feature Selection*. John Wiley & Sons, Inc. DOI: <https://doi.org/10.1002/9780470377888>.
- Ji, Y., Li, N., Cheng, Z., Fu, X., Ao, M., Li, M., Sun, X., Chowwanonthapunya, T., Zhang, D., Xiao, K., Ren, J., Dey, P., Li, X., and Dong, C. (2022). Random Forest Incorporating Ab-Initio Calculations for Corrosion Rate Prediction with Small Sample Al Alloys Data. *NPJ Materials Degradation*, 6, 83. DOI: <https://doi.org/10.1038/s41529-022-00295-5>.
- Jiang, H. (2021). *ML Fundamentals: A Concise Introduction* (1st Ed.). Cambridge University Press. DOI: <https://doi.org/10.1017/9781108938051>.
- Jo, T. (2021). *ML Foundations: Supervised, Unsupervised, and Advanced Learning*. Springer.
- Jung, A. (2022). ML: The Basics, ML: Foundations, Methodologies, and Applications. *Springer Nature Singapore*. DOI: <https://doi.org/10.1007/978-981-16-8193-6>.
- Kokol, P., Kokol, M., and Zagoranski, S. (2022). ML on Small Size Samples: A Synthetic Knowledge Synthesis. *Science Progress*, 105: 003685042110297. DOI: <https://doi.org/10.1177/00368504211029777>.
- Kumar, S., Gaur, V., and Wu, C. (2022). ML for Intelligent Welding and Manufacturing Systems: Research Progress and Perspective Review. *International Journal of Advanced Manufacturing Technology*, 123: 3737–3765. DOI: <https://doi.org/10.1007/s00170-022-10403-z>.

- Kumar, T. P., and Reddy, P. P. (2018). Non-Destructive Analysis of FSW Process and Comparison with Simulation and Microstructural Analysis. *Procedia Manufacturing*, 20: 187–194. DOI: <https://doi.org/10.1016/j.promfg.2018.02.027>.
- Kumpati, R., Skarka, W., and Ontipuli, S. K. (2021). Current Trends in Integration of Nondestructive Testing Methods for Engineered Materials Testing. *Sensors*, 21: 6175. DOI: <https://doi.org/10.3390/s21186175>.
- Lalithakumari, S., and Pandian, R. (2020). Effect of Topology Changes of Neural Network in Classification of Weld Defects. *Materials Today: Proceedings*, 33: 2656–2659. DOI: <https://doi.org/10.1016/j.matpr.2020.01.222>.
- Liu, M., Chen, D., Zhang, Q., Liu, Y., and Zhao, Y. (2022). A Dynamic Multi-Objective Evolutionary Algorithm Assisted by Kernel Ridge Regression. in Q. Xie, L. Zhao, K. Li, A. Yadav, & L. Wang (Eds.), *Advances in Natural Computation, Fuzzy Systems and Knowledge Discovery, Lecture Notes on Data Engineering and Communications Technologies* (Pp. 128–136). Springer International Publishing. DOI: https://doi.org/10.1007/978-3-030-89698-0_14.
- Machado, M. A., Antin, K.-N., Rosado, L. S., Vilaça, P., and Santos, T. G. (2021). High-Speed Inspection of Delamination Defects in Unidirectional CFRP by Non-Contact Eddy Current Testing. *Composites Part B: Engineering*, 224: 109167. DOI: <https://doi.org/10.1016/j.compositesb.2021.109167>.
- Machado, M. A., Rosado, L. F. S. G., Mendes, N. A. M., Miranda, R. M. M., and Dos Santos, T. J. G. (2022). New Directions for Inline Inspection of Automobile Laser Welds Using Non-Destructive Testing. *International Journal of Advanced Manufacturing Technology*, 118: 1183–1195. DOI: <https://doi.org/10.1007/s00170-021-08007-0>.
- Madupu, P., Sk, A., Moses, E. M., and Sreedhar, P. (2017). *Non Destructive Testing for Multipass Gas Tungsten Arc Welding Process for Dissimilar Material 2*, 6.
- Maev, R. Gr., Chertov, A., Scott, R., Stocco, D., Ouellette, A., Denisov, A., and Oberdorfer, Y. (2021). NDE in The Automotive Sector. in N. Meyendorf, N. Ida, N., Singh, R., & Vrana, J. (Eds.), *Handbook of Nondestructive Evaluation 4.0* (Pp. 1–32). Springer International Publishing. DOI: https://doi.org/10.1007/978-3-030-48200-8_21-1.
- Misokefalou, Dr.E., Papoutsidakis, Prof.M., University of West Attica, Priniotakis, Prof.G., University of West Attica, 2022. Non-Destructive Testing for Quality Control in Automotive Industry. *Int. J. Eng. Appl. Sci. Technol.*, 7: 349–355. DOI: <https://doi.org/10.33564/IJEAST.2022.v07i01.054>
- Mookam, N. (2019). Optimization of Resistance Spot Brazing Process Parameters in AHSS and AISI 304 Stainless Steel Joint Using Filler Metal. *Defence Technology*, 15: 450–456. DOI: <https://doi.org/10.1016/j.dt.2019>.
- Nöthen, M. (2021). Applications of NDT 4.0 Cases in Automotive Industry. in N. Meyendorf, N. Ida, R. Singh, & J. Vrana (Eds.), *Handbook of Nondestructive Evaluation 4.0* (Pp. 1–24). Springer International Publishing. DOI: https://doi.org/10.1007/978-3-030-48200-8_52-1.
- Qi, C., Fourie, A., and Zhao, X. (2018). Back-Analysis Method for Stope Displacements Using Gradient-Boosted Regression Tree and Firefly Algorithm. *Journal of Computing in Civil Engineering*, 32: 04018031. DOI: [https://doi.org/10.1061/\(asce\)cp.1943-5487.0000779](https://doi.org/10.1061/(asce)cp.1943-5487.0000779).
- Rodriguez-Galiano, V., Sanchez-Castillo, M., Chica-Olmo, M., and Chica-Rivas, M. (2015). ML Predictive Models for Mineral Prospectivity: An Evaluation of Neural Networks, Random Forest, Regression Trees and Support Vector Machines. *Ore Geology Reviews*, 71: 804–818. DOI: <https://doi.org/10.1016/j.oregeorev.2015.01.001>.
- Rong, Y., Zhang, G., Chang, Y., and Huang, Y. (2016). Integrated Optimization Model of Laser Brazing by Extreme Learning Machine and Genetic Algorithm. *International Journal of Advanced Manufacturing Technology*, 87: 2943–2950. DOI: <https://doi.org/10.1007/s00170-016-8649-6>.
- Sendek, A.D., Ransom, B., Cubuk, E.D., Pellouchoud, L.A., Nanda, J., and Reed, E.J. (2022). ML Modeling for Accelerated Battery Materials Design in The Small Data Regime. *Advanced Energy Materials*, 12: 2200553. DOI: <https://doi.org/10.1002/aenm.202200553>.

- Sevryukov, O.N., Suchkov, A.N., and Guseva, E.V. (2015). Brazing of Modern Engineering Materials with STEMET Amorphous Brazing Filler Metals. *Non-Ferrous Metals*, 45–49. DOI: <https://doi.org/10.17580/nfm.2015.01.12>.
- Shevchik, S., Le-Quang, T., Meylan, B., Farahani, F.V., Olbinado, M.P., Rack, A., Masinelli, G., Leinenbach, C., and Wasmer, K. (2020). Supervised Deep Learning for Real-Time Quality Monitoring of Laser Welding with X-Ray Radiographic Guidance. *Scientific Reports*, 10: 3389. DOI: <https://doi.org/10.1038/s41598-020-60294-x>.
- Shevchik, S.A., Le-Quang, T., Farahani, F.V., Faivre, N., Meylan, B., Zanoli, S., and Wasmer, K. (2019). Laser Welding Quality Monitoring Via Graph Support Vector Machine with Data Adaptive Kernel. *IEEE Access*, 7: 93108–93122. DOI: <https://doi.org/10.1109/access.2019.2927661>.
- Shwartz-Ziv, R., and Armon, A. (2021). *Tabular Data: Deep Learning Is Not All You Need*.
- Siegel, J.E., Beemer, M.F., and Shepard, S.M. (2020). Automated Non-Destructive Inspection of Fused Filament Fabrication Components Using Thermographic Signal Reconstruction. *Additive Manufacturing*, 31: 100923. DOI: <https://doi.org/10.1016/j.addma.2019.100923>.
- Singh, R. (2020). Magnetic Particle Testing, In: *Applied Welding Engineering*. Elsevier, Pp. 331–338. DOI: <https://doi.org/10.1016/b978-0-12-821348-3.00024-0>.
- Siwiec, D., and Pacana, A. (2021). Method of Improve The Level of Product Quality. *Production Engineering Archives*, 27: 1–7. DOI: <https://doi.org/10.30657/pea.2021.27.1>.
- Strehl, A.L., and Littman, M.L. (N.D.). *Online Linear Regression and Its Application to Model-Based Reinforcement Learning* 8.
- Stulp, F., and Sigaud, O. (2015). Many Regression Algorithms, One Unified Model: A Review. *Neural Networks*, 69: 60–79. DOI: <https://doi.org/10.1016/j.neunet.2015.05.005>.
- Vasilev, M., Macleod, C., Galbraith, W., Javadi, Y., Foster, E., Dobie, G., Pierce, G., and Gachagan, A. (2021). Non-Contact In-Process Ultrasonic Screening of Thin Fusion Welded Joints. *Journal of Manufacturing Processes*, 64: 445–454. DOI: <https://doi.org/10.1016/j.jmapro.2021.01.033>.
- Vu, K., Snyder, J., Li, L., Rupp, M., Chen, B. F., Khelif, T., Müller, K.-R., and Burke, K. (2015). *Understanding Kernel Ridge Regression: Common Behaviors from Simple Functions to Density Functionals*.
- Wankerl, H., Stern, M. L., Altieri-Weimar, P., Al-Baddai, S., Lang, K.-J., Roider, F., and Lang, E. W. (2020). Fully Convolutional Networks for Void Segmentation in X-Ray Images of Solder Joints. *Journal of Manufacturing Processes*, 57: 762–767. DOI: <https://doi.org/10.1016/j.jmapro.2020.07.021>.
- Weis, S., Fedorov, V., Elssner, M., Uhlig, T., Hausner, S., Wagner, G., and Wielage, B. (2017). Research Trends in Brazing and Soldering. *Przegląd Spaw. - Welding Technology Review*, 89. DOI: <https://doi.org/10.26628/ps.v89i7.797>.
- Xiao, Z., Song, K.-Y., and Gupta, M. M. (2021). Development of A CNN Edge Detection Model of Noised X-Ray Images for Enhanced Performance of Non-Destructive Testing. *Measurement*, 174: 109012. DOI: <https://doi.org/10.1016/j.measurement.2021.109012>.
- Zhang, Y., and Ling, C. (2018). A Strategy to Apply ML to Small Datasets in Materials Science. *Npj Computational Materials*, 4: 25. DOI: <https://doi.org/10.1038/s41524-018-0081-z>.
- Zhou, B., Svetashova, Y., Byeon, S., Pychynski, T., Mikut, R., and Kharlamov, E. (2020). Predicting Quality of Automated Welding with ML and Semantics: A Bosch Case Study. in *Proceedings of The 29th ACM International Conference on Information & Knowledge Management* (Pp. 2933–2940). Presented at The CIKM '20: The 29th ACM International Conference on Information and Knowledge Management, ACM. DOI: <https://doi.org/10.1145/3340531.3412737>.